Vortex matter in superconductors

V M Pan
National Academy of Sciences of Ukraine

Alexey Pan
University of Wollongong, pan@uow.edu.au

Vortex matter in superconductors

Abstract

The behavior of the ensemble of vortices in the Shubnikov phase in biaxially oriented films of the high-temperature superconductor $YBa_2Cu_3O_{7-\delta}$(YBCO) in an applied magnetic field is investigated for different orientations of the field. The techniques used are the recording of the current–voltage characteristics in the transport current and of resonance curves and damping of a mechanical oscillator during the passage of a transport current. It is shown that the behavior of the vortex ensemble in YBCOfilms, unlike the case of single crystals, is determined by the interaction of the vortices with linear defects—edge dislocations, which are formed during the pseudomorphic epitaxialgrowth and are the dominant type of defect of the crystal lattice, with a density reaching 10^{15} lines/m^2. The effective pinning of the vortices and the high critical current density ($J_c \geqslant 3 \times 10^{10}$ A/m^2 at 77 K) in YBCOfilms are due precisely to the high density of linear defects. New phase states of the vortex matter in YBCOfilms are found and are investigated in quasistatics and dynamics; they are due to the interaction of the vortices with crystal defects, to the onset of various types of disordering of the vortex lattice, and to the complex depinning process. A proposed H−T phase diagram of the vortex matter for YBCOfilms is proposed.

Keywords

matter, vortex, superconductors

Disciplines

Engineering | Physical Sciences and Mathematics

Publication Details

Vortex matter in superconductors

V. M. Pan and A. V. Pan

Vortex matter in superconductors

V. M. Pan[*]

G. V. Kurdyumov Institute of Metal Physics, National Academy of Sciences of Ukraine, bul'var Vernadskogo 36, 03142 Kiev, Ukraine

A. V. Pan[**]

G. V. Kurdyumov Institute of Metal Physics, National Academy of Sciences of Ukraine, bul'var Vernadskogo 36, 03142 Kiev, Ukraine; Institute for Superconducting and Electronic Materials, University of Wollongong, New South Wales 2522, Australia
(Submitted May 18, 2001)

The behavior of the ensemble of vortices in the Shubnikov phase in biaxially oriented films of the high-temperature superconductor $YBa_2Cu_3O_{7-\delta}$ (YBCO) in an applied magnetic field is investigated for different orientations of the field. The techniques used are the recording of the current–voltage characteristics in the transport current and of resonance curves and damping of a mechanical oscillator during the passage of a transport current. It is shown that the behavior of the vortex ensemble in YBCO films, unlike the case of single crystals, is determined by the interaction of the vortices with linear defects—edge dislocations, which are formed during the pseudomorphic epitaxial growth and are the dominant type of defect of the crystal lattice, with a density reaching 10^{15} lines/m^2. The effective pinning of the vortices and the high critical current density ($J_c \geqslant 3 \times 10^{10}$ A/m^2 at 77 K) in YBCO films are due precisely to the high density of linear defects. New phase states of the vortex matter in YBCO films are found and are investigated in quasistatics and dynamics; they are due to the interaction of the vortices with crystal defects, to the onset of various types of disordering of the vortex lattice, and to the complex depinning process. A proposed $H–T$ phase diagram of the vortex matter for YBCO films is proposed. © *2001 American Institute of Physics.* [DOI: [DOI: 10.1063/1.1401182]

INTRODUCTION

It was first shown by the Ukrainian physicist L. V. Shubnikov back in 1936[1] that in superconducting alloys there exists a wide range of magnetic fields at which the Meissner effect gradually diminishes and the magnetic flux penetrates into the volume of the superconductor. In that case the response of the superconductor to an increase in the external magnetic field (i.e., the magnetization curves) have a completely different form than in the case of pure metals, i.e., type-I superconductors. The term "type-II superconductor" was first used for alloys and compounds by Abrikosov in 1957 in developing a consistent theory of type-II superconductors.[2] This theory made it possible to understand the experimental results of Shubnikov on the basis of the concepts of flux quantization and the penetration of magnetic field into type-II superconductors in the form of a lattice of Abrikosov vortices. On the $H–T$ phase diagram (i.e., the diagram in magnetic field versus temperature) the phase in which a type-II superconductor is threaded by vortices— magnetic flux quanta—has ever since that time been called the Shubnikov phase. As time went on, it became clear that vortex states in superconductors are very complex and diverse while at the same time being exceedingly important for understanding the behavior of superconductors in an electromagnetic field and under current loading. A new field of physics has arisen, which might be called vortex-matter physics. In this article we examine the features of the vortex state in films of the moderately anisotropic high-temperature superconductor (HTSC) $YBa_2Cu_3O_{7-\delta}$ (YBCO).

1. QUANTIZED VORTICES IN A SUPERCONDUCTOR

The penetration of magnetic field into a type-II superconductor occurs in the form of quantized vortex lines or flux lines. Each such flux line carries a quantum of magnetic flux, $\Phi_0 = hc/2e = 2.07 \times 10^{-15}$ T·m^2, and has a normal core, which in an isotropic superconductor is a thin normal cylinder along the magnetic field. The radius of this cylinder, the vortex core, is equal to the coherence length ξ (an important scale length in a superconductor, which in the microscopic theory is defined as the distance between interacting electrons in a Cooper pair and in the Ginzburg–Landau (GL) phenomenological theory, as the distance at which the superconducting order parameter varies from its maximum to zero at a superconductor/normal metal boundary).[3] Around the normal core flows an undamped supercurrent, which in isotropic type-II superconductors is oriented in such a way that the magnetic field induced by it is directed along the core and coincides with the direction of the external field. The vortex current flows in a region with a radius of the order of λ, the London penetration depth of a weak magnetic field. For a type-II superconductor this region is much larger than ξ, and this is a consequence of the fact that $\sigma_{ns} < 0$ in a type-II superconductor, i.e., $\lambda \gg \xi$. The penetration of vortices into a type-II superconductor becomes energetically fa-

vorable in an external field $H_{\text{ext}} > H_{c1}$ (H_{c1} is the first, or lower, critical field). Penetrating into the volume of the type-II superconductor, the vortices are spaced a distance $a_0 \propto (\Phi_0/H)^{1/2}$ apart, and when $a_0 \lesssim \lambda$ they begin to interact (repelling each other) owing to the Lorentz force $\mathbf{f}_L = 1/c\,[\mathbf{j} \times \mathbf{\Phi}_0]$, forming a regular triangular lattice in the transverse cross section.[3,4]

2. VORTEX STATE—A NEW FORM OF CONDENSED MATTER

A powerful impulse for the further development of the physics of the vortex state was obtained after the discovery of high-T_c superconductors in 1986. This was because of two important circumstances: first, the critical temperature of HTSC cuprates is so high that they become superconducting at temperatures where thermal fluctuations play an appreciable role, since their energy becomes comparable to the elastic energy of a vortex and/or of the vortex lattice and also to the pinning energy, thus creating the necessary conditions for the appearance of unusual new regions on the $H–T$ phase diagram of the superconductor—different states of the vortex matter and phase transitions between them; second, owing to the layered crystal structure and the anisotropy inherent to HTSC metal-oxide cuprates, favorable conditions are created for the appearance on the $H–T$ diagram of phase regions and phase transitions involving changes in the dimensionality in the vortex ensemble from three-dimensional to two-dimensional and vice versa.

The vortex matter in type-II superconductors is a unique example of a condensed state with controllable parameters.[5] Unlike ordinary condensed-matter systems the density of the constituent particles (magnetic vortices) and their interaction can be changed by several orders of magnitude in a controllable way by simply varying the external magnetic field. In addition, extremely important thermal fluctuation effects in experiments with HTSC cuprates can be observed over a wide temperature range, and these effects are reflected on the $H–T$ phase diagram. Finally, vortex matter is the most convenient tool for studying disordered media—one of the central problems of condensed-matter physics.

In a conventional treatment of the Shubnikov vortex state without allowance for thermal fluctuation and pinning effects, it is assumed that a homogeneous solid vortex-lattice phase exists in the field interval between the lower critical field H_{c1}, where the vortices begin to penetrate into the superconductor, and the mean-field upper critical field H_{c2}, above which the superconductivity vanishes.

The upper critical field $H_{c2}(T)$ of a type-II superconductor is defined as the field at which, at a temperature T, the normal cores of the vortices begin to overlap, and the superconductor becomes "normal." If one ignores thermal fluctuations, then $H_{c2} = \Phi_0/(2\pi\xi^2)$, and this means that a small coherence length is conducive to an increase in H_{c2}.

For high-T_c cuprate superconductors the small value of ξ is the reason why H_{c2} far exceeds 100 T at low temperatures. The well-known $H–T$ phase diagram for a "clean" or ideal type-II superconductor can be obtained using the "mean field approximation" in the GL theory. However, taking thermal fluctuations and disordering effects into account has been

shown to strongly alter the form of this phase diagram, adding new features and new phase regions.

3. THE $H–T$ PHASE DIAGRAM IN THE PRESENCE OF CORRELATED DISORDERING

The presence of linear defects, which by their nature are capable of pinning vortices most strongly along their entire length and whose density is comparable to the density of vortices will give rise to a special state, the so-called "Bose glass," when the vortices are localized in a random manner by linear defects lying parallel to one another. The mechanism of formation of the two-dimensional (or correlated) Bose glass is reminiscent of the mechanism of formation of the three-dimensional vortex glass (which is another disordered state of the vortex lattice, in which it interacts with a set of random pointlike defects of the crystal):[6–10] the linear defects also generate additional low-lying vortex states which differ from those already existing in the perfect lattice, and the vortices are trapped by these states if the potential wells induced by the disorder are sufficiently deep in comparison with the energy of thermal fluctuations. The character of the $H–T$ phase diagram, as in the case of pointlike disorder, is determined by the compensation and competition of the elastic, pinning, and thermal characteristic energies and also by the use of the corresponding Lindemann criterion.[5]

The upward shift of the melting line on the $H–T$ diagram in the presence of linear defects can be estimated, keeping in mind that the modulation of the parabolic elastic potential of the vortex lattice by the linear pinning potential causes an increase in its effective depth. Therefore, in order to remove a given vortex from the confines of the "box," the thermal fluctuations must overcome not only the elastic barrier but also additional pinning barriers. Thus the condition for the loss of stability of the vortex lattice can be determined from the equation

$$k_B T = E_{\text{elastic}} + E_{\text{pin}}, \tag{1}$$

where $k_B T$, E_{elastic}, and E_{pin} are the characteristic energies of thermal fluctuations, the elastic interaction, and pinning. The form of Eq. (1) shows that linear defects are the cause of the shift of the solid↔liquid transition, which in this case is called the Bose glass transition, $H_{BG}(T)$, to higher temperatures in comparison with the melting temperature of the perfect crystal in the absence of these linear defects, $H_{BG}(T) > H_m(T)$.[11] In the case of a fairly low density of linear defects, when the main contribution is given by the elastic energy and the disordering leads only to small shifts of the melting line, the melting of the Bose glass still preserves the features of a first-order transition. Such a transition occurs in low magnetic fields $H < H_\Phi$, where $H_\Phi = \Phi_0/D^2$ is the so-called "matching" field, at which the density of linear defects equals the density of vortices (D is the average distance between linear defects). At higher fields $H > H_\Phi$ the corrections to the melting temperature rapidly decrease, and the melting line of the Bose glass returns to its original position. Thus the greatest deviation of the melting line of the Bose glass from its original position in perfect crystals is expected to occur near $H \cong H_\Phi$.
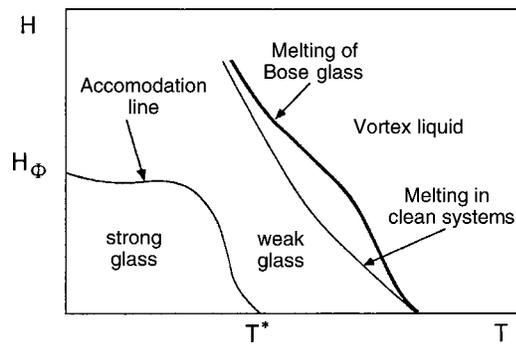
FIG. 1. Schematic $H-T$ phase diagram of the vortex matter in the presence of statistically distributed extended linear (columnar) defects.[5]

FIG. 2. Vortex line in a potential "box" containing an extended linear defect,[5,10,11] which modulates the parabolic potential well, creating new minima and displacing the vortex from its equilibrium position in the box. Also shown are the short-wavelength lateral displacements that arise due to the simultaneous action of a random point potential. These displacements promote depinning of the vortex from the linear defect.

Figure 1 shows a schematic phase diagram of a vortex system with correlated disorder arising because of the presence of defects. According to Ref. 5, an accomodation line separates two regimes of behavior of the vortex matter: the regime of individual pinning, and the regime of collective pinning with the participation of linear defects.[11] The position of the accomodation line is determined by the competition and compensation of the characteristic elastic energy arising because of the interaction with the remaining vortex lattice (the potential box) and the pinning energy. Below the accomodation line the pinning force dominates, and the vortices can therefore be shifted substantially from their equilibrium positions in the perfect lattice. To emphasize the particularly strong individual pinning in such a state, it has been proposed[5] to call this state of the vortex lattice a "strong Bose glass." It was proposed[5] that the state that is formed in the collective pinning regime be considered a quasilattice or "weak Bose glass." A very important distinction between the effect of linear and point defects is that, unlike point defects, which stimulate lateral (bending) deformations of the vortices, linear pinning centers *stabilize* the residence of a given vortex line in the potential box formed by the elastic interaction with the neighbors against thermal fluctuations and against bending displacements caused by point defects (as is shown schematically in Fig. 2), thereby preventing the formation of a three-dimensionally disordered solid state of the vortex lattice. It is particularly important to emphasize that in the case of linear crystal defects—pinning centers—the "strong" glass phase, with a highly two-dimensional distorted structure of the vortex lattice and the highest critical current density, occupies the low-field part of the $H-T$ phase diagram. Of course, such behavior contrasts with the effects of point disorder, when the more strongly pinned three-dimensionally disordered solid vortex phase appears in higher fields.[12–18]

Thus it turns out that the contributions of linear and point defects to the volume pinning force not only do not add together but they may even subtract, i.e., the point disorder promotes the depinning (breakaway) of vortex lines from linear defects. This conjecture has been shown experimentally[12–18] to be well confirmed for configurations in which the linear defects are oriented parallel to the magnetic field (or, more precisely, to the direction of the vortex lines). Since all real HTSC materials unavoidably contain pointlike defects (e.g., oxygen vacancies), the question of the dominant pinning mechanism is one of paramount impor-
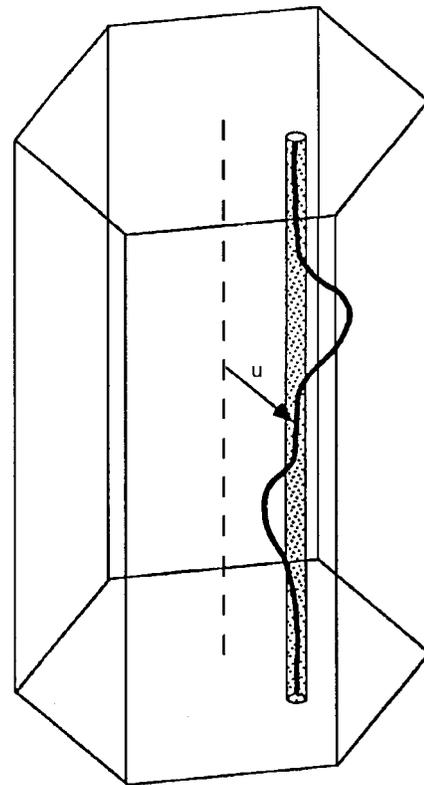
tance for the controlled creation of desired transport current-carrying properties of a material. The competition of these two types of disorder was first studied experimentally in Refs. 12–18 and theoretically in Ref. 19. In particular, it was shown in Ref. 19 that in the real cases the influence of the correlated disorder is dominant in the behavior of the vortex matter, even when the density of defects is lower than the density of vortices.

Up till now, however, the discussions and calculations of theorists have been based exclusively on the hypotheses of structures with linear defects obtained in HTSCs subjected to irradiation by heavy ions with high energies (around 1 GeV and higher). Very recently it has become clear that dislocation ensembles in strongly biaxially textured epitaxial films of YBCO play the role of strongly-pinning correlated linear defects.

4. PINNING CENTERS IN EPITAXIAL YBCO FILMS

As we have said, the fact that the highest J_c ($\geqslant 10^{10}$ A/m^2 at 1 T and 77 K) can be obtained relatively easily in YBCO epitaxial films while remaining unachievable for any YBCO bulk materials should be attributed to features of the defect structure of the films and, accordingly, to the formation of a volume pinning force in them due to the most effective interaction, primarily with linear defects. Many attempts have been made to establish a linkage of the pinning force to the the screw dislocations that initiate the corresponding three-dimensional mode of film growth during

deposition (by the appearance and propagation of screw dislocations)—the so-called ''screw-mediated'' growth[20,21]—and to the growth steps on the surface of the film in the two-dimensional, ''layer-by-layer,'' growth mode. However, these attempts have been futile: for example, one can prepare films in which the concentration of screw dislocations will differ by an order of magnitude or more (from 5×10^7 to 10^9 cm^{-2}) while the critical current density will be the same, and vice versa. Moreover, the cores of the growth screw dislocations in YBCO films have been shown by electron microscope studies to have a characteristic transverse size that is much greater than the coherence length.[22] Therefore, they can hardly be effective pinning centers. The experimental evidence[13,14,23–25] of a very high density of edge dislocations in YBCO epitaxial films is also not very convincing, since the investigators could scarcely believe that a dislocation line (i.e., the core of a dislocation) could in itself serve as a strong pinning center providing effective ''core pinning.'' Indeed, on the one hand, back in the early papers of Dew-Hughs[26] it was shown that dislocations pin only when they comprise an ensemble which forms ''walls'' of a cellular structure in metallic bcc alloys owing to the long-range stress fields, which can lead to both δl and δT_c pinning.[6] As to an isolated linear defect, in the papers by Dew-Hughes and his followers it was clearly stated that ''isolated dislocations lead to a negligibly small change in κ_{GL}'' (the parameter of the Ginzburg–Landau theory). And, on the other hand, it is known from the theory of dislocations that the transverse cross section of the core can have an area of the order of the square of the Burgers vector, which is clearly much smaller than the square of the coherence length, even for HTSCs ($\xi_{ab} \approx 1.5$ nm for YBCO in comparison with the value of the Burgers vector $B \approx 0.4$ nm). Thus it appears that, as in the case of point defects, dislocations can pin only collectively, since the depth of the pinning potential well U_p is small, and the experimental pinning force of an individual dislocation, $f_p = dU_p/dr$, is small. Two new important results have played a most important role in the further development of the concepts of dislocation pinning in HTSCs, presenting unambiguous evidence in favor of strong pinning on dislocation lines. The first of these was obtained by Chisholm and Smith,[27] and then, more convincingly, by Merkle and co-workers.[28,29] A high-resolution transmission electron microscope (HRTEM) was used to obtain pictures of the real distribution of atoms inside and in a neighborhood around the core of a complete [001] edge dislocation. It was found that the core of an edge dislocation is a highly distorted structure on a characteristic scale length of the order of 5–10 interatomic distances, i.e., around 3 nm.[28,29] In addition, it was found that in the core region there is an excess of copper above stoichiometry (see, e.g., Ref. 28). Thus it turns out that the cores of dislocation lines have a structure that resembles that of artificial defects introduced by irradiation with heavy ions of high energy; those defects act as exceedingly strong one-dimensional linear pinning centers. This has been shown convincingly in many studies (see, e.g., Refs. 30–32).

It remained to show whether a structure state providing a very high average dislocation density is formed in YBCO epitaxial films during their deposition and growth. It appears
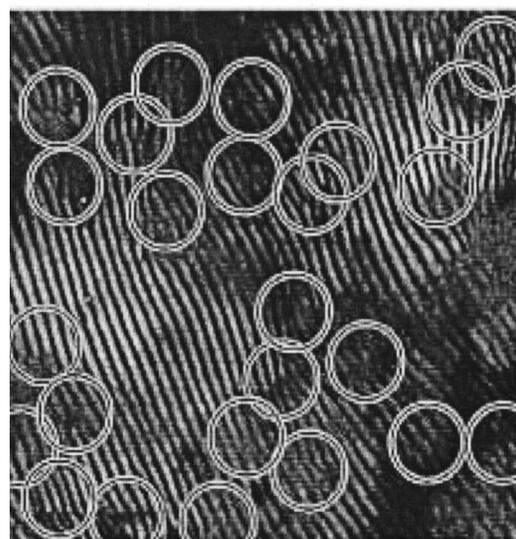
FIG. 3. a—Moiré pattern showing edge dislocations with the aid of a transmission electron microscope (TEM); the dislocation line are perpendicular to the cuprate planes. The dislocations, which are additional crystallographic half planes in the structure are clearly revealed by the moiré fringes, the distance between which is 2.2–2.3 nm.[13,14,18,25,35] b—TEM moiré pattern showing the distribution of edge dislocations (in a YBCO film 10–12 nm thick, deposited on a single-crystal MgO substrate); the dislocation lines are perpendicular to the ab plane. The arrangement of the dislocations corresponds to an averaged misorientation angle of 1.2° between neighboring domains (subgrains).[13,14,18,25,35]

that our recent HRTEM results (some of which are shown in Fig. 3) unambiguously confirm the formation of such a dislocation structure in YBCO films exhibiting record values of $J_c(H)$. These results also make it possible to understand the mechanism of formation of linear defects during deposition and growth of the films. The problem of the formation of a dislocation substructure during epitaxial growth of films in general and YBCO films in particular goes beyond the scope

of the present paper, and for an introduction to this topic the reader is referred to the recent papers cited as Refs. 13, 14, 18, 20–25, 27–29, 33, and 34.

5. DYNAMICS OF VORTICES IN A YBCO SUPERCONDUCTOR WITH LINEAR PINNING CENTERS

It follows from the results of structural studies[13,14,18,20–25,27–29] that the most interesting type of defects in YBCO thin epitaxial films and bicrystals in respect to their contribution to the pinning and dynamics of vortices are low-angle tilt dislocation boundaries. Of course, point defects (oxygen vacancies) distributed in a random manner, dislocation loops due to stacking faults and lying parallel to the ab plane, and {110} microtwins are present in the films, and in certain cases make an appreciable contribution to the behavior of the vortices and to the magnetic-field dependence of the critical current density.

As we have said, recent transport measurements in combination with a scaling analysis provide substantial arguments in favor of the existence of a Bose glass phase in YBCO crystals and thin films irradiated by heavy ions at high energy (1 GeV and higher). The formation of a Bose glass phase is initiated by randomly distributed correlated extended defects—columnar tracks made by the heavy ions. However, as we have seen above, correlated linear defects in deposited YBCO thin films are actually distributed nonuniformly: they form more or less well-formed rows or walls of edge dislocation lines lying parallel to one another, with nonsuperconducting cores of transverse size $D \approx \xi_{ab}$. The dislocation walls frame domains of mosaicity, azimuthally misoriented by approximately 1° with respect to the neighboring domains. Inside the domains the dominant pinning defects are pointlike (oxygen vacancies). For such a spatial distribution of correlated linear pinning centers the Bose glass phase exists only at sufficiently low applied magnetic fields, for which $a_0 \propto (\Phi_0/H)^{1/2}$ remains much larger than the transverse domain size L_{domain}. When the magnetic field is increased to a certain critical value $H_{B \to F}$ there is a crossover to a distinctive new correlated glassy state, the "Fermi glass," in which the vortices are located both in dislocation walls and in the interior of the domains. The vortices inside the domains interact with random point defects, and their behavior is therefore similar to that in single crystals.

At a certain value of the applied magnetic field the linear tension of the vortex "softens" as a result of dispersion of the elastic constant $C_{44}(\mathbf{k})$, and then the picture arises that is described below in an analysis of the concrete results of our recent experimental measurements of $J_c(H,T,\theta)$ for YBCO films (θ is the angle between the cuprate planes and the applied magnetic field H). For an idealized case, i.e., when the low-angle boundary is formed by a regular row of equally spaced edge dislocations parallel to one another and with no other disruptions of the crystalline order in neighboring subgrains (domains), one can use the model of vortex dynamics. For this case Kasatkin[35–37] examined the transport of vortices along low-angle domain walls (or more precisely, bicrystal boundaries). In the framework of this model it was shown that despite the strong single-particle core pinning by lines of edge dislocations, the motion of the vortices occurs along the domain walls in accordance with the conventional

ideas.[32,38,39] The model is actually completely adequate for treating the electrodynamics of bicrystals with this sort of tilt boundaries and with small values of the misorientation angle. The model does not require making any sort of assumptions as to the transmissivity for supercurrent or to Josephson properties of the bicrystals with such a tilt dislocation boundary, as must be made for the models proposed in Refs. 40–43. Most importantly, in the framework of the model one can consistently explain the strong dependence of the critical current J_c through the boundary on the misorientation angle ϑ between the adjacent domains ("banks" of the junction), as has been observed for YBCO bicrystals and films.[35–37,44] In order to apply this model for describing polydomain mosaic films containing this sort of low-angle boundaries, one must take into account the additional effects in the motion of vortices in both the direction transverse to the domains and along the curved domain walls, with spatial variation of the misorientation and also of the distance between adjacent dislocations.

The model of vortex transport along a row of edge dislocations lying parallel to the c axis and forming, as we have said, a low-angle boundary between slightly misoriented subgrains (domains) is based on the above treatment of the pinning and dynamics of vortices in superconductors with extended linear (columnar) defects.[11,32,35–38] It is important to note that collective effects were not taken into account, at least not in Refs. 35–37. According to the results of those papers, the depinning of vortices residing at linear pinning centers and their subsequent dynamics in the presence of transport current occur owing to the spontaneous formation of vortex excitations caused by thermal fluctuations in the volume of the superconductor. A vortex excitation has the form of a partially depinned vortex loop (Fig. 2). When the size of the depinned part of such a loop exceeds a certain critical value for a given superconducting transport current (see Refs. 35 and 36), the loop becomes unstable and begins to expand until it touches the neighboring linear defect. After that, the motion of the remaining part of the given vortex will occur through the motion of two vortex "steps" (kinks) moving apart in opposite directions along the c axis under the influence of the Lorentz force. The model of vortex motion along an equidistant row of mutually parallel dislocations can be extended to the case of a real polydomain (mosaic) structure of a film with a low-angle-boundary network formed by ensembles of edge dislocations, as appears to be the case in an actual image similar to that shown in Fig. 3. These dislocations are found in a more or less disordered state and are not equidistant, as was proposed above. Nevertheless, using a percolation approach, as was done by Gurevich in a treatment of flux creep,[45,46] one expects that the low-angle boundaries will serve as percolation channels for the thermally activated motion of vortices. This is apparently the case, since the activation energy $U_c(D)$ for the transition of a vortex from one edge dislocation to a neighboring one [i.e., at a distance $D(\vartheta)$] is much less than the corresponding value U_{c0} for the traversal of a vortex across a domain. Thus the network of low-angle boundaries can be formed by a spatial landscape of U_c, in the more or less pronounced "valleys" of the vortex activation energy $U_c(r)$. Considering the thermally activated flux flow (TAFF) regime
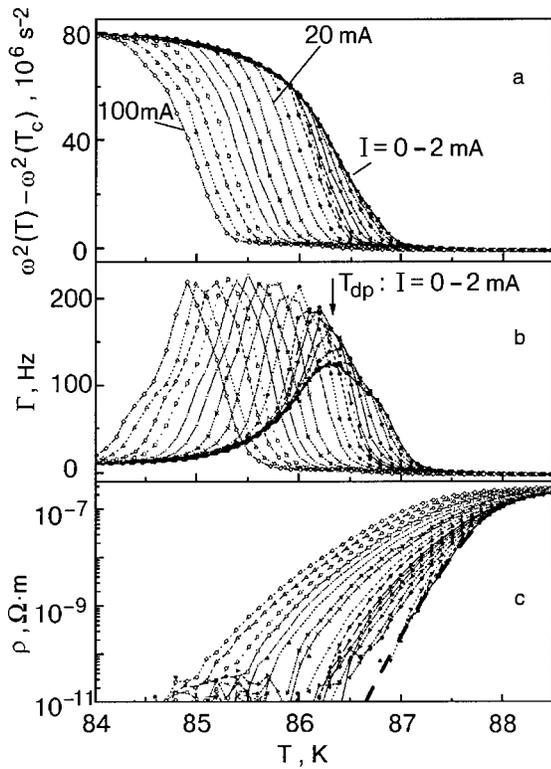
FIG. 4. Square of the resonance frequency (a), of the corresponding damping (b), and of the resistivity (c) as functions of temperature for different values of the transport current at a field $H = 2$ T and $\theta = 0°$. The dashed curve in part (c) is an example of a resistivity curve rescaled by means of Eq. (2) to the diffusion constant, which was taken for calculation of the damping curve (see Fig. 5) according to Eq. (3).

FIG. 5. Damping curves for $I = 0$ and 100 mA at $H = 2$ T. The dotted and dashed curves were calculated according to Eq. (3), following the procedure described in Refs. 48, 52, and 58.

of vortex motion along these percolation channels, one expects that the average distance between nearest dislocations is nevertheless related to the angle of misorientation of neighboring domains. Then at small values of the angle one has $\vartheta \langle U_c(D) \rangle \propto \langle (\sin \vartheta)^{-1} \rangle$, and, hence, the strong dependence $J_c(\vartheta)$ obtained for a straight row of equidistant dislocations will hold for the percolation situation with $\sin \vartheta$ replaced by its value averaged over the whole film.

A strong dependence $J_c(\vartheta)$ for polydomain epitaxial films of YBCO with low-angle boundaries was observed experimentally in Ref. 47.

5.1. Dynamic depinning of the vortex lattice in YBCO films

An extremely informative method for describing the behavior of the vortex ensemble in YBCO films in the dynamic regime utilizes a mechanical oscillator with a high Q factor under passage of a dc transport current. Such measurements have been done using miniature current and potential contacts on a vibrating YBCO film sample.[48] The technique permits making the following simultaneous measurements: 1) the change in the square of the resonance frequency, $\omega^2(B_a, T) - \omega^2(0, T)$, of a mechanical oscillator with a film sample of the HTSC YBCO attached to it, executing vibrational motion in a magnetic field, which yields information about the pinning force[49,50] (Fig. 4a); 2) the damping Γ, which characterizes dissipative processes in the sample in connection with the motion of the vortices[49,50] (Fig. 4b); 3) the resistivity of YBCO films (Fig. 4c). Using this technique we were able to study the dynamic behavior of vortices in
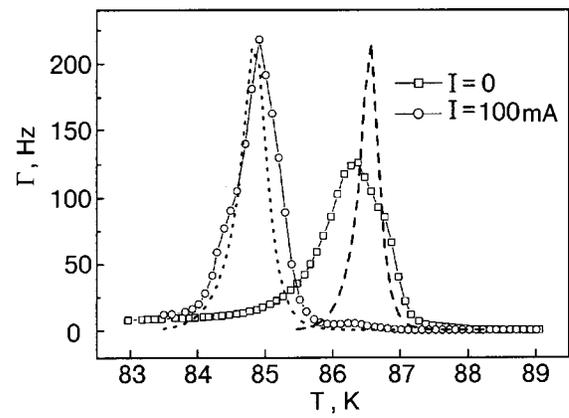
YBCO films in the region of their depinning at angles $\theta = 90°$ (which is equivalent to a parallel orientation of the applied field relative to the cuprate planes), $75°$, and $60°$, with the transport current always flowing perpendicular to the applied field.

The dynamic behavior of the vortices in such an oscillator is well described by a *diffusion model* for the thermally activated vortices.[50] In this model the diffusion constant is given by

$$\mathcal{D} = \mathcal{D}(H, T) = \rho(H, T)/\mu_0, \tag{2}$$

where ρ is the resistivity of flux flow. In the framework of this model, in accordance with Refs. 48, 51, and 52, the damping of the vibrating superconductor has the form

$$\Gamma = \frac{1}{2I_i \omega} \left(\frac{\mu_0 H^2}{2} \right) V_p \chi''(\mathcal{D}), \tag{3}$$

where I_i is the effective moment of inertia of the oscillator, which can be found experimentally,[48] ω is the resonance frequency of the oscillator, V_p is the volume of the sample, and χ'' is the imaginary part of the ac susceptibility of the sample: χ'' as a function of temperature has a maximum $\chi''_{max} = 0.41723$.[51] This result is valid for any value of the transport current density J, i.e., χ''_{max} is independent of the current load. Changing the diffusion parameter $\mathcal{D}$ by the passage of current only shifts the position of the damping peak (e.g., on account of the dependence of the effective activation barrier U_p on the current), but it does not introduce any changes in its absolute value. It should be noted that the top of the damping peak determines the position of the depinning temperature T_{dp} or the irreversibility point.

If the measured value of the resistivity $\rho(T, H, J)$ is used for $\mathcal{D} = \rho/\mu_0$ according to the procedure described in Ref. 48, then it becomes possible to apply the theory quantitatively to the discussion of the experimental results, through the use of Eq. (3). Figure 5 shows the the calculated damping curves for two values of the current $I = 0$ mA ($J = 0$ A/m^2) and $I = 100$ mA ($J \approx 2 \times 10^8$ A/m^2). The calculated temperature dependence for $\Gamma(I = 100$ mA), its absolute value, and the width of the transition turn out to be in good agreement with experiment. Furthermore, it is clear that richer information about the depinning transition of the vortex lattice can

be obtained from the damping of a vibrating superconductor than from the value of the electric field induced by the motion of the vortex lattice. The broadening and asymmetry of the damping peak are evidence of a diverse character of the depinning of the vortex lattice.

Of course, from the present investigations it is difficult to reconstruct the microscopic picture of the dynamics of the moving vortices, but, considering the known results from observations of the motion of an almost ordered vortex lattice in superconducting crystals,[53] the results of theoretical papers on moving disordered vortex lattices,[54,55] and the aforementioned complex "valley" spatial landscape of the pinning potential U_p in real YBCO superconducting films, we propose a scenario that will lead to the observed effects (Fig. 4b): 1) a narrowing and symmetrizing of the damping peak upon application of a current load; 2) a rise of the peak value of the damping for $J > 2 \times 10^6$ A/m^2. We note that at high values of the transport current density the height of the damping peak becomes independent of the current density, and only the position of the peak changes, shifting to lower temperatures with increasing current.

In the YBCO films under study there is a chaotic distribution of the pinning potential, the interaction with which leads to disordering of the vortex lattice. The situation become even more complicated when one takes into account that rather complex vortex configurations can arise for field orientations close to parallel with respect to the ab planes, when two mutually perpendicular vortex subsystems can co-exist simultaneously in the superconducting films on account of the two components of the field vector penetrating into the film.[56–58] Then for vortices parallel to the ab plane the majority of linear defects are dislocation loops distributed chaotically in the interior of the film. Their characteristic size is 5–7 nm, but then their pinning force hardly decreases with temperature because of the weak stress–strain fields near the core (see Sec. 7) and also because in this orientation the bending modulus C_{44} does not "soften" along the field, as it does in the case $H\|c$ on account of the anisotropy and layered nature of the atomic structure. In the case of vortices parallel to the c axis there exists a hierarchy of pinning centers, with a spatial distribution: 1) the strongest obstacles for the transverse motion of the vortices are close-packed dislocation walls with vortices already residing on them and with shielding currents flowing along these walls; 2) individual "standing" or "threading" dislocations, which are also strongly pinning if $H\|c$; 3) point defects inside the domains, which can rapidly decrease the net pinning force and current density, as follows from the arguments given above (see Sec. 3) and the experimental data presented below (Sec. 8).

The larger-scale topological defects existing in YBCO films, such as shaped (polygonized) domain dislocation walls, can lead to plastic flow of vortex rows but not to displacement of an elastically deformable vortex lattice. A mechanism for the motion of vortices along so-called "easy-slip channels" has been proposed previously (see, e.g., Ref. 59). However, this mechanism requires a small shear modulus C_{66} in the vortex lattice, and that ordinarily takes place in fields approaching H_{irr}. Thus the thermally activated depinning of the vortex lattice under the influence of a small driving force can occur near $H_{irr}(T)$ along "plastic flow
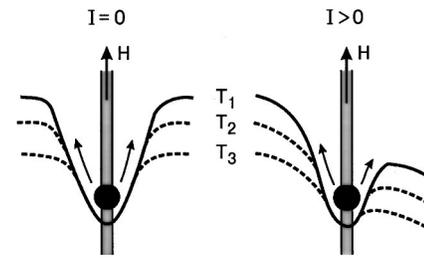

FIG. 6. Pinning potential with a vibrating vortex at different temperatures ($T_1 < T_2 < T_3$) during the passage of current and with no current.

valleys," i.e., the easy-slip channels, when they are oriented parallel to the driving force (see also Ref. 60). This behavior, as we have said, can be treated as percolational.[45,46] If the initial breakaway of the vortices when depinning is achieved is interpreted as vortex rows moving along "channels," then one expects that the vortex lattice inside the domains remains pinned on account of the strong pinning on domain walls perpendicular to the driving force, i.e., it remains practically immobile at temperatures $T < T_{dp}$. As the temperature is raised, the observed damping peak at $T_{dp}(J=0)$ is indicative of depinning of strongly pinned regions. Under the influence of the aforementioned factors, this peak, which characterizes the depinning of the vortex lattice, becomes broad and asymmetric.

Phenomenologically, without specifying the type of pinning defects, one can describe the behavior of the damping peak of a vibrating sample at $J=0$ by introducing a distribution of the potential energy of the activation barriers. Such a distribution will lead to two main effects: broadening of the transition with respect to temperature, and, consequently, decreasing the height of the damping peak at the depinning temperature. Indeed, the use of a single-barrier approximation in the framework of the diffusion model leads to an unavoidable difference between theory and experiment, as is usually observed in practice.[48,52]

One can give a simple picture in which the loading of the sample by current leads to tilting of the whole pinning potential[61] and in which the depth of the potential is temperature dependent (Fig. 6). By scanning the pinning potential well with the aid of low-amplitude mechanical vibrations of the superconducting sample, one can record the tiniest changes in the height of this well at very low transport currents. This effect is observed at current densities as low as $J < 10^6$ A/m^2. The decrease and shift of the high-temperature part of the transition (Fig. 4) indicates that the upper part of the potential distribution (high U_p) is shifted to lower values of U_p. It is possible that a decrease and shift to higher values of U_p occurs in the low-lying part of the U_p distribution (i.e., at lower temperatures). This effect can scarcely be observed by the technique used, since the flux bundles remain pinned by the highest potential barriers until the temperature becomes high enough to provoke depinning.

At large values of the driving force ($J \gg 10^6$ A/m^2) the velocity of the vortices is expected to play the role of an order parameter. The observed motional narrowing of the damping peak upon increasing current loading (i.e., driving force) means that a new "instrument" for the ordering of the vortex lattice has appeared. We again note the explicit satu-
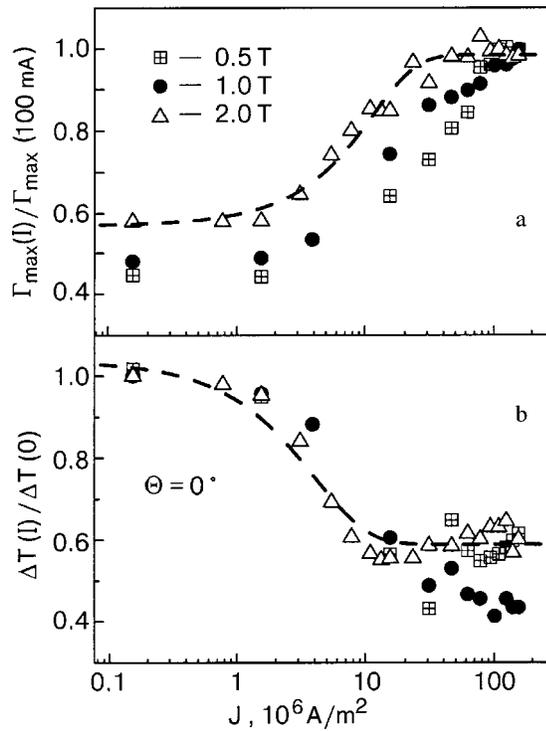
FIG. 7. Normalized damping peak (a) and the half-width of the damping peak (b) of a vibrating YBCO film as functions of the transport current density at different values of the external magnetic field. The dashed curves were calculated with the use of the function $a + b\tanh(J/c)$, where $a = 0.57$ (1.03), $b = 0.42$ (0.44), and $|c| = 15 \times 10^6 (5.5 \times 10^6)$ A/m^2 for the upper (lower) panel.

FIG. 8. a—Resistivity of a YBCO film versus the transport current density, measured at $H = 2$ T and various temperatures with a step of 0.1 K. The dotted line is the so-called "vortex glass" transition at a temperature $T_g = 86.35$ K. b—Scaling behavior of the $\rho(J)$ curves as described in the text; here $z \approx 1.7$ and $\alpha = 4.7 \pm 1$.

ration effect at high values of the transport current (Fig. 7). In terms of the picture of a distribution of effective potential barriers, this result indicates that the moving elastic vortex lattice becomes increasingly dominant over the pinning disorder and approaches a delta-function distribution of barriers. In other words, the thermally activated depinning behaves as if all the barriers have equal depth. It can also be assumed that the vortex lattice begins to behave like an elastically deformable continuum whose motion is insensitive to the individual pinning centers. An important circumstance is that the damping $\Gamma(T)$ of the vibrating film can be described quantitatively with the help of formula (3) without any free parameters by using the experimentally determined resistivity of the flux flow as the diffusion constant (2).

5.2. Vortex glass or depinning?

Simultaneous measurements of the resonance frequency and damping of a vibrating sample of a superconducting YBCO film together with the resistivity curves $\rho(T,J)$ (Fig. 4) permit a direct comparison of the so-called "glass temperature" T_g and the depinning temperature T_{dp}. Figure 8a shows the dependence of the resistivity on the transport current density. It is seen that the $\rho(J)$ curves are clearly separated into two groups by the dotted line $T_g = 86.35$ K. Behavior of this type is often used as an argument in favor of the possibility of a "vortex glass" state.[7,8,62] In other words, it is assumed that the vortex lattice undergoes a second-order phase transition to a "vortex glass" state at a temperature T_g.
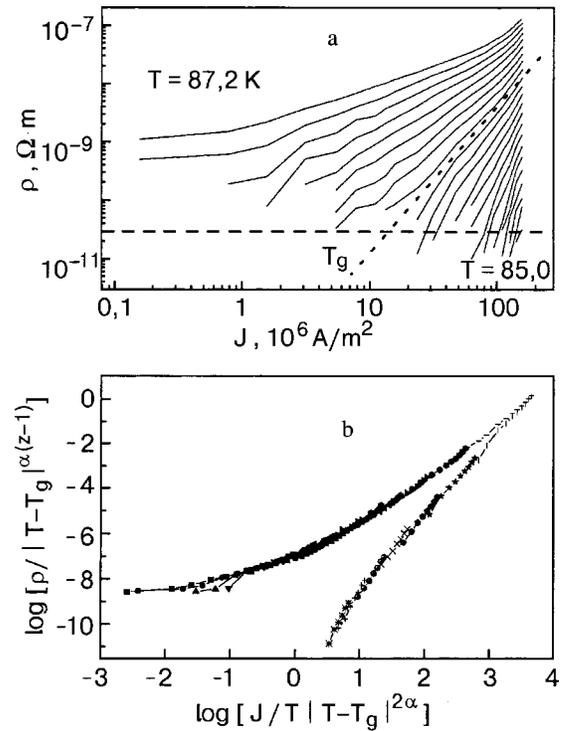
The "vortex glass" model predicts that the typical scaling procedure can be applied to the $\rho(J)$ curves to give two groups of lines with different signs of the curvature. Indeed, the experimental curves can be subjected to a scaling analysis in the coordinates $\rho_{ab}/|T-T_g|^{\alpha(z-1)}$ versus $J/T|T-T_g|^{2\alpha}$, where $z = 1.7 \pm 0.15$ and $\alpha = 4.7 \pm 1$ (Fig. 8b). Both parameters agree with the values given in Refs. 63 and 64.

A particularly interesting fact that emerges from these measurements is that for $I = 0$ and angles $\theta = 90°$, $75°$, and $60°$ in magnetic fields of 0.5 T $\leq H \leq 2$ T the depinning temperature and the temperature of the proposed formation of the "vortex glass" coincide: $T_g \cong T_{dp}$. Since the behavior observed with the use of the mechanical oscillator can be described by a depinning transition in the framework of diffusion concepts, it is necessary to understand to what extent the result obtained from the scaling analysis can be taken as evidence of a second-order phase transition in the vortex lattice. In contrast to the experimentally proven melting of the vortex lattice, which has been observed in clean high-temperature superconductors by different techniques, the "vortex glass" transition is determined solely by means of the scaling analysis shown in Fig. 8b. One wonders whether the result of this scaling analysis can be described using a different model without invoking the concepts of a "vortex glass" and a phase transition of the vortex lattice into such a state.

Indeed, a serious alternative interpretation of the results of the scaling analysis of the experimental data is the percolation model of vortex motion proposed by a number of authors over the past few years.[65–67] According to the percolation model, a superconductor found in the mixed state con-
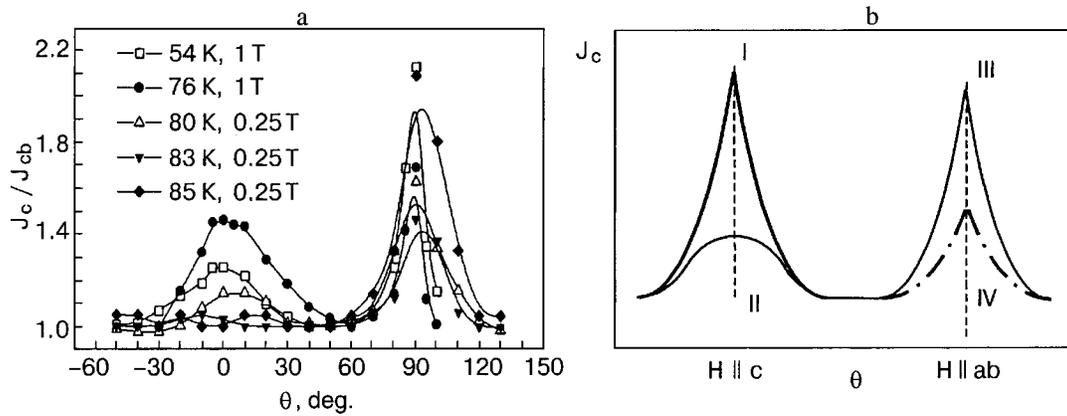
FIG. 9. a—Angle dependence of $J_c(H)$ measured by the four-probe transport method for YBCO films deposited by a pulsed laser technique on a LaAlO$_3$ substrate. b—Schematic representation of the angle dependence of $J_c(H)$ for the case when both dislocation ensembles perpendicular and parallel to the ab plane contribute to the two-peak curves: the contributions from linear defects (I), from the intersection of vortices with dislocations (II), from pinning centers lying in the ab plane (III), and from the anisotropy of H_{irr} (IV).

sists of percolation regions with different resistivities, which correspond to pinned and free (depinned) vortex lines. When the percolation threshold is reached there is a transition from the depinned state to a pinned state with an insignificant linear resistivity. In the framework of the percolation picture the disorder and the distribution of percolation regions also leads to a broader pinning transition. Consequently, the narrowing of the depinning transition when a current load is applied, as we have said, can be interpreted as a decrease of the disorder (or the pinning) of the vortex lattice as a result of its motion. In the ''microscopic'' picture of this process, the vortex lattice, as its velocity increases, ceases to ''notice'' the point and pointlike defects (e.g., the crossing of dislocation lines by vortices), through which a vortex passes in a very short time. There is insufficient time for the vortex to interact with them, since the pinning time is shorter than the

relaxation time of the vortex lattice (the increasing velocity the lattice becomes ''stiffer''). On the whole, this process leads to an average viscosity η of the vortex lattice which is related to the diffusion constant as $\mathcal{D} = \mu_0 H^2/\eta$.

6. THE $J_c(H,T,\theta)$ CURVES FOR YBCO FILMS. RELATION TO THE CHARACTERISTIC ENSEMBLE OF LINEAR DEFECTS

Saemann-Ischenko[68] was the first to show that when the magnetic field vector is rotated with respect to the c axis (while maintaining constancy of the Lorentz force) in a biaxially textured epitaxial YBCO film the $J_c(H,T,\theta)$ curves have two characteristic peaks at $H\|c$ ($\theta=0°$) and $H\|ab$ ($\theta=90°$), which are shown in Fig. 9 (our data). The prop-

TABLE I. Properties, characteristics, and behavior of the $J_c(\theta)$ peaks.

Experimentally measured parameter	$J_c(\theta)$ peak for $H\|c$	$J_c(\theta)$ peak for $H\|ab$
1. Temperature change during measurements	Relative height grows with increasing T for 40–80 K, then the peak is suppressed for $T \to T_{irr}(H)$.	Relative height decreases with increasing T, but for $T \to T_{irr}(H)$ the peak becomes dominant.
2. Influence of the strength of the applied magnetic field	Practically vanishes in fields above 2–3 T.	The higher the field, the sharper the peak. For $T \to T_{irr}(H)$ only this peak remains.
3. Rate and method of deposition of the film	Low-rate off-axis magnetron sputtering tends to enhance the peak (e.g., for sapphire/CeO$_2$/YBCO films).	High-rate pulsed laser deposition substantially enhances this peak.
4. Effects of the substrate and buffer layers	The greater the misfit of the crystal lattices between the materials of the substrate, buffer layers(s), and YBCO film, the stronger the peak.	This peak is sharper and more significant if the misfit is small, as, e.g., for substrates of SrTiO$_3$ or LaAlO$_3$.
5. Influence of deposition temperature of YBCO film	Height increases with increasing T (up to 745–750 °C) for sapphire/CeO$_2$/YBCO films.	Substantially suppressed with increasing T (up to 745–750 °C) in the case of sapphire/CeO$_2$/BCO films.
6. Effect of a change in thickness of the YBCO film	The thicker the YBCO film (at least on a LaAlO$_3$ substrate), the higher the peak.	Practically independent of the thickness of the YBCO film.
7. Effect of a change in the growth mode of the YBCO film	2D growth mode suppresses the peak and 3D mode enhances it.	3D growth mode leads to substantial suppression of the peak.

erties, characteristics, and behavior of the two peaks are described below and listed in Table I.

It can be seen from Table I that the relative height of these peaks depends on the conditions of measurement of the current–voltage characteristics and determination of the value of the critical current, specifically, on the temperature of the measurements, the applied magnetic field, and the value of the electric field E_c. Indeed, the $J_c(H)$ peak for $H\|c$ initially grows with increasing temperature approximately from 40 to 80 K and then, when the temperature approaches the line of irreversibility, the J_c peak is substantially suppressed and can even vanish in the case of YBCO films deposited by pulsed laser sputtering on $LaAlO_3$ substrates. On the contrary, the $J_c(H)$ peak for $H\|ab$ survives at all temperatures, magnetic fields, and velocities of the vortex lattice under the influence of the Lorentz force.

As is now known from the high-resolution electron microscopy data, there are several types of dislocation ensembles that can form in YBCO films during their growth:

1. Misfit edge dislocations at the boundary due to the usual mismatch of the interatomic spacings in the crystal lattices of the substrate and growing film.

2. Dislocation loops due to the existence of stacking faults (i.e., the local appearance of "extra" or "missing" segments of CuO_2 planes, usually up to 10 nm in size, during growth); these are edge dislocations, the dislocation lines being parallel to the ab plane.[69]

3. "Threading" edge dislocations, whose dislocation lines, being parallel to the c axis and perpendicular to the surface of the film, as a result of the polygonization process partially or completely form low-angle tilt boundaries of domains of azimuthal mosaicity in the film. The average density of such dislocation lines can reach 10^{11} lines/cm^2 and even higher.[13,14,18,23–25,31] These dislocations are formed mainly as a result of the realization of a two-dimensional heteroepitaxial growth mode in which a so-called "rotational" relaxation of the misfit at the boundary occurs. In particular, this mechanism can be enhanced further on account of specific growth conditions, e.g., as a consequence of their rotational misfit on the R plane of sapphire and the (001) plane of CeO_2 (for details see, e.g., Refs. 70 and 71).

4. Screw dislocations at the boundary in low-angle twist boundaries, which are a source of screw dislocations in the low-angle domain walls, making them increasingly more complex tilt–rotational boundaries the higher the degree of mismatch of the crystal lattices at the boundary. Screw dislocation sources emerging on the surface of the film at higher deposition temperatures (above 740 °C for YBCO) can initiate a three-dimensional growth mechanism with the formation of polygonal spirals.[20,25,35,72]

Analysis of the data obtained as a result of measurements of the angle dependence of $J_c(H)$ for a large number of perfect biaxially textured YBCO films with high $J_c(H)$ shows convincingly that the maxima of the critical current and hence the orientation of the dislocation ensemble correspond to two directions: parallel to the c axis, and parallel to the ab plane. This conclusion is equivalent to the assumption that the effective pinning of vortices in YBCO films is due to extended linear defects oriented along the given directions, i.e., dislocation ensembles **a** [100] and dislocations and loops
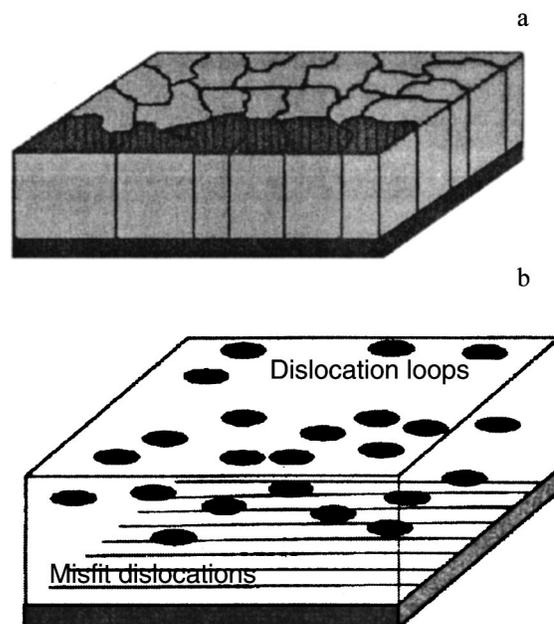
FIG. 10. Schematic illustrations of ensembles of edge dislocations, which are formed in YBCO films during growth in different modes: a—ensembles of "threading" dislocations perpendicular to the cuprate planes and lying in low-angle tilt domain boundaries (substrate with large misfit (MgO, YSZ, sapphire+CeO_2)); b—ensembles of dislocations parallel to the cuprate planes and consisting of misfit dislocations at the boundaries and dislocation loops induced by local stacking faults (substrate with small misfit ($SrTiO_3$, $LaAlO_3$)).

lying in the ab plane. It is important to note that these latter dislocations and loops also contribute to the maximum $J_c(H\|c)$, since, as was first shown in Ref. 73 and then confirmed by the present authors in Refs. 12–14, 74, and 75, when the vortices are parallel to the c axis they can interact with transverse dislocation lines as with pointlike defects. Then the function $J_c(H,\theta)$ has a domelike character of the type $J_c(\theta)\propto(\cos\theta)^{1/2}$. It can also be assumed that some contribution to the volume pinning force is made by point defects such as oxygen vacancies. At the peak $J_c(H\|c)$ the two contributions from point and quasi-point pinning centers create the pedestal that vanishes as the line of irreversibility is approached, i.e., for $T\rightarrow T_{irr}(H)$, as the magnetic field is increased, and as the velocity of the vortices (i.e., the dimensionless number E_c) increases.[12–14,18] As to the peak $J_c(H\|ab)$, since it survives at all temperatures, fields, and velocities of the vortex lattice, we may assume that it is due to dislocation pinning on dislocations and loops lying in the ab plane and also to anisotropy of $H_{irr}(T)$. As was discussed above, anisotropy of $H_{irr}(T)$ leads to anisotropy of the resistivity due to the motion of the vortex lattice under the influence of the Lorentz force. This means that at a given value of E_c the value of J_c determined from the current–voltage characteristics for $H\|ab$ and $H\|c$ will be substantially different.

Thus, in considering the behavior of YBCO films one should keep in mind that there are two ensembles of edge dislocations: 1) with dislocation lines along the c axis, and 2) in the ab plane. This was confirmed in our recent papers[74–77] by means of transmission and high-resolution electron microscopy and also by electronic transport measurements of the angle dependence of the critical current density in a magnetic field. Such measurements have also been made by other
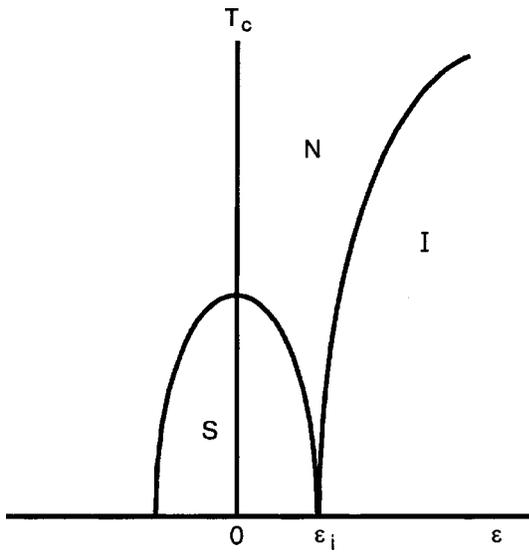
FIG. 11. Schematic phase diagram of an anisotropic metal-oxide cuprate of the YBCO type with a high T_c. This diagram was obtained by Gurevich and Pashitskii[82] from the well-known $T_c(x)$ phase diagram, where x is the doping level, with the use of Eq. (4).

groups.[68,78] For a clearer and more convincing demonstration of the real nonuniform distribution of dislocation ensembles in YBCO films prepared under different conditions of nucleation and growth and by different growth mechanisms, in Fig. 10 we show schematic illustrations of the fine structure of the films: with a set of mosaic domains differing from one another by low-angle tilt dislocation boundaries (a typical misorientation angle of around $1-2°$, typical domain size of $20-50$ nm, average distance between dislocations in the boundary $10-20$ nm, and average dislocation density around 10^{11} lines/cm^2 (Fig. 10a); with misfit dislocations at the boundary and dislocation loops due to stacking faults, i.e., with extra or missing segments of the copper–oxygen layers of the CuO_2 type,[69] with the dislocation lines lying in the ab plane and an extremely high average dislocation density (Fig. 10b). It is surprising that in YBCO films such a dislocation structure with a high density can coexist with a very high degree of perfection of the crystal structure, as characterized by transmission and high-resolution electron microscopy[23–25,27–29] and x-ray diffractometry.[74] However, the most reliable tool for experimental observation of these two different dislocation ensembles is measurement of the angle dependence of $J_c(H, \theta)$ at a constant value of the Lorentz force[74–77] (see Fig. 9).

7. ELASTIC STRAIN FIELDS IN THE NEIGHBORHOOD OF LINEAR DEFECTS AND THE FEATURES OF THE PINNING POTENTIAL IN YBCO FILMS

It has been shown experimentally[79–81] that layered anisotropic HTSC metal-oxide cuprates have an anomalously strong anisotropic dependence of the critical temperature T_c on the pressure in the case of uniaxial compression. For example,[80] for the optimally doped $YBa_2Cu_3O_{7-\delta}$ single crystal the derivatives $\partial T_c / \partial P_i$ measured along the principal crystallographic axes are: $\partial T_c / \partial P_a \approx -(1.9-2)$ K/GPa, $\partial T_c / \partial P_b \approx (1.9-2.2)$ K/GPa, and $\partial T_c / \partial P_c \approx -(0-0.3)$ K/GPa. This means that the pressure dependence $T_c(P)$ for

an isotropically, hydrostatically compressed crystal is very weak. However, in regions of the crystal with a local anisotropic deformation the changes of T_c can be significant. In the linear approximation this dependence can be written as

$$T_c(\mathbf{r}) = T_{c0} - C_{ik}\varepsilon_{ik}(\mathbf{r}). \tag{4}$$

Here T_{c0} is the critical temperature of the undeformed crystal, ε_{ik} is the strain tensor, and the coefficients $C_{ik} = -\partial T_c / \partial \varepsilon_{ik}$ are related to the derivatives $\partial T_c / \partial P_a$ (Fig. 11). According to Refs. 79 and 81, the diagonal coefficients C_{ii} in the ab basal plane of the crystal are $C_a = -\partial T_c / \partial \varepsilon_{aa} \approx -220$ K, $C_b = \partial T_c / \partial \varepsilon_{bb} \approx 320$ K, and $\partial T_c / \partial \varepsilon_{cc} \approx 0$.

Based on the experimental data,[79–81] a theoretical calculation by Gurevich and Pashitskii[82] showed that the elastic deformations created by a single edge dislocation or a dislocation ensemble (e.g., a "wall" of dislocations) in an anisotropic crystal can cause a local elevation or depression of T_c and can even suppress the superconducting state completely at a given temperature (e.g., at 77 K). Consequently, the region of the normal (nonsuperconducting) phase should exist around a dislocation core, which, as described above in accordance with the data of Refs. 28 and 29, is (for a "threading" edge dislocation $\mathbf{a}$ [100]) a cylindrical channel of highly plastically deformed medium with a diameter of around 2 nm. The normal regions surrounding the core should also play an important role in the formation of the pinning potential of the superconductor. Therefore it is necessary to examine in more detail the deformation mechanism of suppression of superconductivity in the neighborhood of a dislocation core, i.e., of the effect of an elastic strain field in the anisotropic crystal $YBa_2Cu_3O_{7-\delta}$.

An edge dislocation perpendicular to the ab plane gives rise to elastic strains in the ab plane and to corresponding local changes in T_c. Under certain conditions, if the Burgers vector $\mathbf{B}$ is directed at an angle ϑ to either the a or b axis, the change of T_c is given by the expression

$$\delta T_c = -C[\varepsilon + \beta(\varepsilon_{xx} - \varepsilon_{yy})\cos 2\vartheta + 2\beta\varepsilon_{xy}\sin 2\vartheta], \tag{5}$$

where

$$\varepsilon = \varepsilon_{xx} + \varepsilon_{yy}; C = \frac{C_a + C_b}{2}; \beta = \frac{C_a - C_b}{C_a + C_b}. \tag{6}$$

Using the well-known[83] components of the strain tensor ε_{ik} under the condition $\mathbf{B} \| \mathbf{a}$, Pashitskii[74] obtained an expression for the variation of the critical temperature in cylindrical coordinates:

$$\delta T_c(r, \varphi) = -\frac{CB}{2\pi(1-\sigma)} \frac{\sin\varphi}{2}[(1-2\sigma) + 2\beta\cos^2\varphi]. \tag{7}$$

Here φ is the azimuthal angle in the ab plane, measured from the a or b axis, $\sigma \approx 0.28$ is Poisson's ratio,[84] and B is the modulus of the Burgers vector, which is approximately equal to the lattice constant $a \approx 0.4$ nm in the ab plane. Thus Pashitskii[74] determined the boundary of the region of the normal phase around a dislocation core, i.e., the region in which the local value of T_c is lower than the characteristic average level:

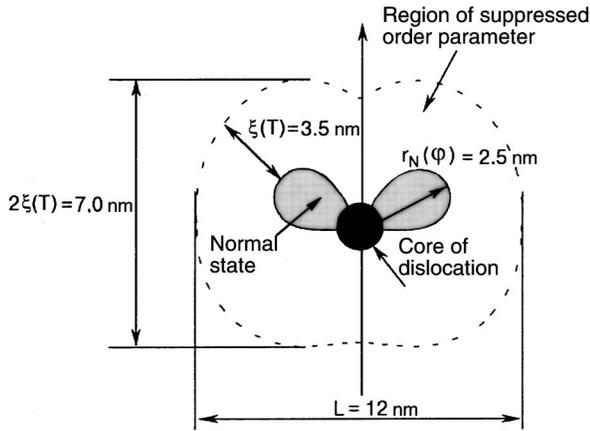$$r_N(\varphi, T) = R_0(T)\sin\varphi[1 + \beta_0\cos^2\varphi] \geq 0, \tag{8}$$

FIG. 12. Shape and size of the region of the normal state at 77 K, and also the region partially suppressed superconducting order parameter in the neighborhood of a dislocation core for a "threading" dislocation whose dislocation line is perpendicular to the ab plane of the YBCO crystal; calculated by Pashitskii[74] with the use of Eqs. (4), (7), and (8).

where

$$R_0(T) = \frac{CB(1-2\sigma)}{2\pi(1-\sigma)T_{c0}\tau}, \quad \tau = 1 - \frac{T}{T_{c0}}, \quad \beta_0 = \frac{2\beta}{1-2\sigma}. \tag{9}$$

For $T_{c0} = 90\,\text{K}$ and for the values of the coefficients $C_{a,b}$ mentioned above, the parameter $R_0(T) \approx 0.042/\tau\,(\text{nm})$, and $\beta_0 \approx -24$. At $T = 77\,\text{K}$ we have $R_0 \approx 0.3\,\text{nm}$ and the maximum of r_N occurs in the direction $\varphi = -\pi/4$ and has the value $r_{N\,\text{max}} \approx 2.5\,\text{nm}$ (Fig. 12).

If now we take into account the proximity effect, then it becomes clear that the region with a suppressed superconducting order parameter extends in all directions to a distance of the order of the coherence length $\xi(T) = \xi_0/\tau^{1/2}$ (where $\xi_0 \approx 1.3\,\text{nm}$ is the coherence length at $T = 0$).

At 77 K we have $\xi(T) \approx 3.5\,\text{nm}$, and the maximum width of the normal region is $L(T) = 2[r_{N\,\text{max}} + \xi(T)] \geq 12\,\text{nm}$. The area of the region of suppressed order parameter per dislocation parallel to the c axis can be estimated as $S_N(T) \approx 2\xi(T)L(T) \approx 8 \times 10^{-13}\,\text{cm}^2$ at 77 K. This means that at a concentration of edge dislocations of around $10^{11}\,\text{lines/cm}^2$ the fraction of the normal phase is approximately equal to 10%. Each component of the function $L(T)$ increases at a different rate as $T \to T_{c0}$: $r_N(T) \propto \tau^{-1}$, and $\xi(T) \propto \tau^{-1/2}$. Consequently, the width and shape of the pinning potential well change with increasing temperature faster than τ^{-1}, the dependence approaching $\tau^{-3/2}$ as $T \to T_{c0}$. Although a detailed analysis of the consequences of this situation goes beyond the scope of this paper, there are sufficient grounds for assuming that the pinning force arising in the interaction of vortices with dislocations of this ensemble should decrease appreciably with increasing temperature, as is observed in the measurement of the temperature dependence of $J_c(H \| c)$ (Fig. 13).

We conclude this Section by noting that the anisotropy parameter β_0 in Eq. (8) for dislocation lines parallel to the ab plane is smaller by many times than that for perpendicular "threading" dislocations, because of the neglibibly small value of C_c. In this case $\beta = 2/(1-2\sigma) \approx 4.5$. Thus one can assume that the dislocations and dislocation loops lying par-
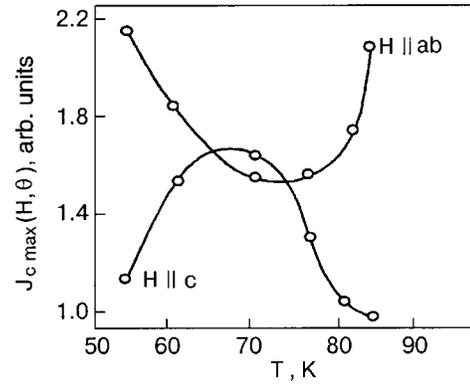

FIG. 13. Temperature dependence of the height of the $J_c(H,\theta)$ peaks for orientations of the magnetic field $H \| c$ and $H \| ab$, shown in relative units in relation to the position of the pedestal (or "background").

allel to the ab plane, unlike the perpendicular ones, have insignificant strain fields in the neighborhood of the core. This means that the corresponding pinning potential wells are much narrower and steeper. The elementary pinning force for these dislocations is larger. In addition, their shape is apparently weakly dependent on temperature, and hence the pinning force is independent of temperature, as is confirmed in experiment (Fig. 13). The opposite forms of the temperature dependence of the relative height of the J_c peaks for $H \| ab$ and $H \| c$ is evidently due in large measure to the fact that the pinning potential wells have a different shape and different temperature behavior: steeper slopes and weak temperature dependence for $H \| ab$, and more gradual slopes and strong temperature dependence for $H \| c$.

8. MAGNETIC FIELD DEPENDENCE OF $J_c(H)$ AND THE H–T PHASE DIAGRAM FOR AN ANISOTROPIC HTSC WITH LINEAR DEFECTS FOR $H \| c$

The typical $J_c(H)$ curves of YBCO films for $H \| c$, as was shown in Refs. 74–77, 85, and 86 have three different segments (Fig. 14). The low-field part is a plateau or a weakly field-dependent part up to the point $H = H_A$, which corresponds to $a_0 \approx (\Phi_0/H_A)^{1/2} \approx \lambda_L$ ($\sim 0.1\,\text{T}$ at 77 K), where the position of the points H_A must be determined as the intersection of the horizontal part of the curve $J_c(H) \approx \text{const}$ with the extrapolated part $J_c \propto H^{-0.5}$, but on our curves (Fig. 14) this cannot always be done because of the lack of measurements in sufficiently low fields. Undoubtedly
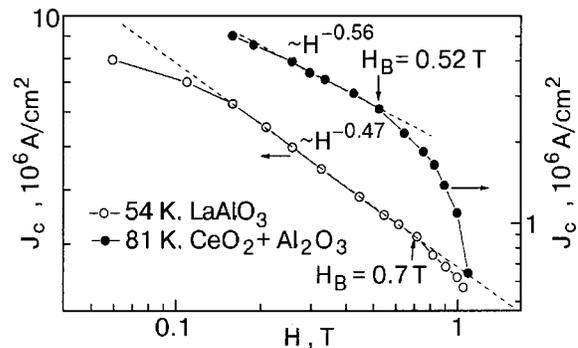

FIG. 14. Magnetic-field dependence for biaxially oriented epitaxial YBCO films for $H \| c$.

here we are dealing with a regime of individual or single-particle pinning, in which the vortices are far apart and non-interacting, and a vortex lattice is not formed. This effect was also mentioned in Refs. 85 and 86, but the authors explained it as a transition through a so-called "matching" field $H = H_\Phi$, at which the density of vortices becomes equal to the density of linear pinning defects parallel to them. This is clearly incorrect for two reasons: first the authors of Refs. 85 and 86 incorrectly determined the density of defects from the etch pits, obtaining a value too low by one or two orders of magnitude ($10^8 - 10^9$ lines/cm^2 instead of the actual $10^{10} - 10^{11}$ lines/cm^2, as is shown in Refs. 23–25); second, as the "matching" field is approached in YBCO, it is known[87] that $J_c(H \| c)$ increases rather than remaining constant.

The intermediate part of the field dependence of $J_c(H \| c)$ turns out to be practically linear on a log–log scale: $J_c \propto H^{-q}$, where the exponent q is close to 0.5. Such a dependence can be the result of the presence of a two-dimensional correlated "quenched" disorder in the vortex lattice, apparently of the Bose glass type, in this interval of fields ($H_A < H < H_B$). At higher fields ($H > H_B$) the $J_c(H)$ curve begins to decrease faster, viz., as H^{-q} with $q = 1.0 - 1.5$.

A tentative explanation for this is that the vortex lattice begins to interact with random pointlike defects as well. Indeed, at the crossover field H_B the intervortex distance $a_0 \approx (\Phi_0 / H_B)^{1/2}$ becomes comparable to the transverse size L_d of the domains of mosaicity, which are slightly misoriented with respect to one another and are separated by low-angle dislocation boundaries. This is the most important point in this treatment, since at low fields ($H_A < H < H_B$) the vortex lattice "perceives" the network of threading dislocations as a random, chaotic system which induces a quasi-two-dimensional correlated state of the vortex lattice of the Bose glass type with a high value of the bending modulus C_{44}. When the field increases to H_B, some of the vortices no longer have a chance to become pinned on the dislocation lines in the low-angle boundaries, since the benefit in terms of the pinning energy would be much smaller than the energy cost due to the 2D deformation of the vortex lattice. As a result, a significant number of vortices are inside the domains, being only weakly pinned by pointlike defects. Since the magnetic field in this case is already quite high, one expects that a substantial change in behavior will occur, much as in the case of single crystals. Thus one expects an intradomain crossover from 2D to 3D behavior of the vortex lattice due to wave-vector dispersion of the bending modulus $C_{44}(\mathbf{k})$ of the vortex lattice, which is interacting with a random pointlike pinning potential. However, because of this the phenomena that occur are radically different from that which occurs in a single crystal. In a single crystal the vortices, by "softening," more easily adjust to the chaotically distributed point centers, and the resulting bulk pinning force increases, and $J_c(H)$ also increases from 10^8 to 5×10^8 A/m^2 (Refs. 12–18). In this case the vortices are pinned (while $H \lesssim H_B$) on linear defects, and $J_c(H) = 5 \times 10^9 - 10^{10}$ A/m^2. Therefore, when some vortices are found inside the domains and become unstable to lateral deformations owing to the sharp decrease of their effective linear tension, $J_c(H)$ does not increase but instead begins to fall.
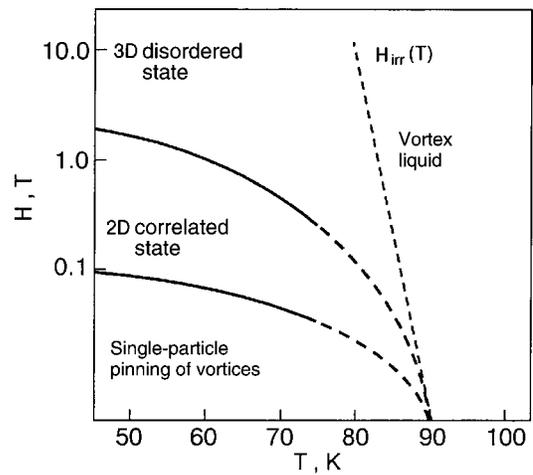

FIG. 15. Proposed $H-T$ phase diagram of the vortex matter in a YBCO epitaxial film for $H \| c$.

This crossover in the behavior of the vortex system can be classified as a manifestation of a change in dimensionality in the nonuniform ensemble. We denote the nonuniform state of the vortex ensemble, interacting with the 2D pinning potential parallel to equidistant linear centers forming a polygonal 2D lattice (if the field is applied parallel to the c axis),[74–77] as a correlated inhomogeneous Bose glass (CIBG). This state differs substantially from the usual state of a triangular vortex lattice and a random Bose glass, in which the linear pinning centers are distributed chaotically. The CIBG state (which is realized for $H_A < H < H_B$) also differs from the nonuniform state of the vortex lattice formed for $H > H_B$, where the vortices interact with both linear and planar defects. The latter can be called a Fermi glass, since the relation between the number of vortices resident on dislocations and the number of vortices inside the domains can be found by introducing a distribution of the Fermi type, much as was done by Gurevich.[45,46] Figure 15 shows the proposed $H-T$ phase diagram of the states of the vortex lattice in a YBCO film for a magnetic field direction $H \| c$.

CONCLUSIONS

—Several type of dislocations and dislocation ensembles are formed in YBCO films during their growth: 1) edge dislocations of nonregistry at the boundary; 2) dislocation loops due to stacking faults (i.e., with extra or missing segments of the CuO$_2$ planes), the lines of which are parallel to the ab plane; 3) edge dislocations in low-angle boundaries of mosaic domains with a density of up to 10^{11} lines/cm^2 and higher.

—The efficient pinning of vortices and high critical current densities ($J_c \gtrsim 3 \times 10^{10}$ A/m^2 at 77 K) in epitaxial YBCO films are due to the high density of linear defects formed in the process of nucleation and growth of the film.

—The "motional narrowing" of the damping peak is indicative of *ordering* of the vortex lattice upon the passage of current. The remarkable agreement between the measured damping peak and the theoretical curve obtained in the framework of the diffusion model attests to preservation of a

gradual transition (*the absence of sharp phase transformations*) upon the depinning of the vortices in systems with strong disorder.

—The *"vortex glass" transition* temperature obtained by means of scaling of the resistivity coincides with the depinning temperature measured at zero current, indicating that the interpretation of this transition is ambiguous and might be explained in terms of a model of vortex depinning.

—Linear defects oriented along the c axis, i.e., dislocation ensembles **a** [100], are the reason for the appearance of the $J_c(H\|c)$ peak, while dislocations and loops lying in the ab plane contribute to the peak $J_c(H\|ab)$ and also to the peak $J_c(H\|c)$ as a result of the interaction of vortices with transverse dislocation lines as with pointlike defects.

—Opposite temperature behavior of the peaks of $J_c(H,\theta)$ for $H\|c$ and $H\|ab$ is found experimentally. The peak $J_c(H\|c)$ initially grows with increasing temperature and then is suppressed when T approaches $T_{irr}(H)$. In contrast, the relative height of the peak $J_c(H\|ab)$ becomes larger and larger as the temperature increases. This behavior is due to the different temperature dependence of the different contributions to $J_c(H\|c)$ and $J_c(H\|ab)$: pinning on dislocations, pinning on pointlike defects, and the effect of the anisotropy of the strain fields near the dislocation cores.

—In the neighborhood of the cores of edge dislocations whose lines are parallel to the c axis a strain field arises which plays an important role in the formation of the pinning potential and the local suppression of the superconducting order parameter and T_c. For $T<T_c$ this will give rise to anisotropic regions of the normal phase near the dislocation core.

—In the neighborhood of dislocation lines parallel to the ab plane no appreciable strain fields appear. It can be assumed that this is the cause of the opposite behavior of the pinning force and critical current density in the case $J_c(H\|ab)$.

—The measured $J_c(H)$ curves for $H\|c$ in YBCO films demonstrate two clear crossovers, corresponding to transitions from $J_c(H)\sim$ const at low fields, in which the vortex lattice has not yet formed and the interaction of vortices with linear centers occurs in the regime of individual pinning, to $J_c\propto H^{-0.5}$ at intermediate fields (the motion of the vortex lattice as a deformable 2D continuum) and, finally, to $J_c\propto H^{-q}$ (where $q\sim 1-1.5$) at higher fields.

—The inhomogeneous state of a vortex ensemble interacting with an ensemble of parallel equidistant linear centers which are arranged in a network substantially differs from the state of a random 2D Bose glass.

[*]E-mail: pan@imp.kiev.ua
[**]E-mail: pan@uow.edu.au

[1] L. V. Shubnikov, V. I. Khotkevich, Yu. D. Shepelev, and Yu. N. Ryabinin, Zh. Éksp. Teor. Fiz. **7**, 221 (1937).

[2] A. A. Abrikosov, Zh. Éksp. Teor. Fiz. **32**, 1442 (1957) [Sov. Phys. JETP **5**, 1174 (1957)].

[3] V. V. Shmidt, *Introduction to the Physics of Superconductors* [in Russian], Nauka, Moscow (1982), p. 240.

[4] U. Essman and H. Träuble, Phys. Lett. A **24**, 526 (1967).

[5] V. Vinokur, B. Khaykovich, E. Zeldov, M. Konczykowski, R. A. Doyle, and P. H. Kes, Physica C **295**, 209 (1998).

[6] G. Blatter, M. V. Feigel'man, V. B. Geshkenbein, A. I. Larkin, and V. M. Vinokur, Rev. Mod. Phys. **66**, 1125 (1994).

[7] M. P. A. Fisher, Phys. Rev. Lett. **62**, 1415 (1989).

[8] D. S. Fisher, M. P. A. Fisher, and D. A. Huse, Phys. Rev. B **43**, 130 (1991).

[9] A. E. Koshelev and V. M. Vinokur, Preprint cond-mat/9801144 (January 14, 1998).

[10] G. W. Crabtree and D. R. Nelson, Phys. Today **50**, 38 (1997).

[11] D. R. Nelson and V. M. Vinokur, Phys. Rev. B **48**, 13060 (1993).

[12] V. F. Solovjov, V. M. Pan, and H. C. Freyhardt, Phys. Rev. B **50**, 13724 (1994).

[13] V. M. Pan, V. F. Solovjov, A. L. Kasatkin *et al.*, in *Physics and Materials Science of High Temperature Superconductivity IV*, Vol. 26 of NATO ASI Series, edited by R. Kossowsky *et al.*, Kluwer Academic Publ., Dordrecht, Boston, London (1997), p. 3.

[14] V. M. Pan, in *Physics and Materials Science of Vortex States, Flux Pinning and Dynamics*, Vol. 356 of NATO ASI Series, edited by R. Kossowsky *et al.*, Kluwer Academic Publ., Dordrecht, Boston, London (1999), p. 1.

[15] V. M. Pan, V. F. Solovjov, and H. C. Freyhardt, in *Advances in Cryogenic Engineering, Materials*, Vol. 42, edited by L. T. Summers, Plenum Press, New York (1997), p. 663.

[16] V. M. Pan, V. F. Solovjov, and H. C. Freyhardt, Physica C **279**, 18 (1997).

[17] V. M. Pan, V. F. Solovjov, and H. C. Freyhardt, Czech. J. Phys. **46**, 1643 (1996).

[18] V. M. Pan, Usp. Fiz. Met. **1**, 49 (2000).

[19] T. Hwa, D. R. Nelson, and V. M. Vinokur, Phys. Rev. B **48**, 1167 (1993).

[20] J. Mannhart, D. Anselmetti, J. G. Bednorz *et al.*, Semicond. Sci. Technol. **5**, 125 (1992).

[21] D. G. Schlom, D. Anselmetti, J. G. Bednorz *et al.*, Z. Phys. B: Condens. Matter **86**, 163 (1992).

[22] V. L Svetchnikov, Met. Phys. Adv. Tech. (2001), in press.

[23] S. K. Streiffer, B. M. Lairson, C. B. Eom *et al.*, Phys. Rev. B **43**, 13007 (1991).

[24] S. J. Pennycook, M. F. Chisholm, D. E. Jensson *et al.*, Physica C **202**, 1 (1992).

[25] V. Svetchnikov, V. Pan, Ch. Traeholt, and H. Zandbergen, IEEE Trans. Appl. Supercond. **AS-7**, 1396 (1997).

[26] V. Narlikar and D. Dew-Hughes, Phys. Status Solidi **6**, 383 (1964).

[27] M. F. Chisholm and D. A. Smith, Philos. Mag. A **59**, 181 (1989).

[28] Y. Gao, K. L. Merkle, G. Bai, H. L. M. Chang, and D. J. Lam, Physica C **174**, 1 (1991).

[29] K. Merkle, Interface Sci. **2**, 311 (1995).

[30] V. Hardy, J. Provost, D. Groult *et al.*, J. Alloys Compd. **195**, 395 (1993).

[31] S.-W. Chan, J. Phys. Chem. Solids **55**, 1415 (1994).

[32] D. R. Nelson and V. M. Vinokur, Phys. Rev. Lett. **68**, 2398 (1992).

[33] A. Gervais and D. Keller, Physica C **246**, 29 (1995).

[34] Z. L. Wang, D. H. Lowndes, D. H. Christen, D. K. Kroeger, C. E. Klabunde, and D. P. Norton, Physica C **252**, 125 (1995).

[35] V. M. Pan, A. L. Kasatkin, V. L. Svetchnikov, and H. W. Zandbergen, Cryogenics **33**, 21 (1993).

[36] V. M. Pan, A. L. Kasatkin, and H. C. Freyhardt, IEEE Trans. Appl. Supercond. **AS-7**, 1588 (1997).

[37] A. L. Kasatkin and V. M. Pan, *The Ninth International Workshop on Critical Currents*, IWCC 9-99, Extended Program Book, July 7–10, 1999, The Pyle Center, University of Wisconsin-Madison, USA (1999), p. 14.

[38] E. H. Brandt, Phys. Rev. Lett. **69**, 1105 (1992).

[39] V. M. Pan, V. A. Komashko, V. S. Flis, A. L. Kasatkin, V. L. Svetchnikov, O. P. Karasevskaja, A. G. Popov, A. V. Pronin, C. L. Snead, M. Suenaga, and H. W. Zandbergen, Physica B **284–288**, 831 (1999).

[40] J. Mannhart, J. Supercond. **3**, 281 (1990).

[41] R. Gross and B. Mayer, Physica C **180**, 235 (1991).

[42] P. A. Nilsson, D. Winkler, J. A. Alarco *et al.*, Appl. Phys. Lett. **59**, 3030 (1991).

[43] D. Shi, Appl. Supercond. **1**, 61 (1993).

[44] D. Dimos, P. Chaudhari, and J. Mannhart, Phys. Rev. B **41**, 4038 (1990).

[45] A. Gurevich, H. Kuepfer, and C. Keller, Semicond. Sci. Technol. **4**, 91 (1991).

[46] A. Gurevich, Phys. Rev. B **42**, 4857 (1990).

[47] M. Strikovsky, G. Linker, S. V. Gaponov *et al.*, Phys. Rev. B **45**, 12522 (1992).

[48] A. V. Pan, F. Ciovacco, P. Esquinazi, and M. Lorenz, Phys. Rev. B **60**, 4293 (1999).

[49] P. Esquinazi, J. Low Temp. Phys. **85**, 139 (1991).

[50] M. Ziese, P. Esquinazi, and H. F. Braun, Semicond. Sci. Technol. **7**, 869 (1994).

[51] E. H. Brandt, Phys. Rev. Lett. **68**, 3769 (1992).

[52] M. Ziese, P. Esquinazi, Y. Kopelevich, and A. B. Sherman, Physica C **224**, 79 (1994).

[53] F. Pardo, F. de la Cruz, P. Gammel, E. Bucher, and D. J. Bishop, Nature (London) **396**, 348 (1998).

[54] P. Le Doussal and T. Giamarchi, Phys. Rev. B **57**, 11356 (1998).

[55] S. Scheidel and V. Vinokur, Phys. Rev. B **57**, 2574 (1998).

[56] L. N. Bulaevskii, M. Ledvij, and V. G. Kogan, Phys. Rev. B **46**, 366 (1992).

[57] A. V. Pan, R. Hohne, M. Ziese, P. Esquinazi, and C. Assmann, in *Physics and Materials Science of Vortex States, Flux Pinning and Dynamics*, Vol. 356 of NATO Science Series, edited by R. Kossowsky *et al.*, Kluwer Academic Publ., Dordrecht, Boston, London (1999), p. 545.

[58] A. V. Pan, PhD thesis, University of Leipzig, Leipzig (2000).

[59] V. M. Pan, G. G. Kaminsky, A. L. Kasatkin, M. A. Kuznetsov *et al.*, Supercond. Sci. Technol. **5**, 48 (1992).

[60] H. Jensen *et al.*, Phys. Rev. Lett. **60**, 1676 (1988); Phys. Rev. B **38**, 9235 (1988).

[61] A. V. Pan, P. Esquinazi, and M. Lorenz, Phys. Status Solidi B **215**, 573 (1999).

[62] E. H. Brandt, Rep. Prog. Phys. **58**, 1465 (1995).

[63] R. H. Koch, V. Foglietti, W. J. Gallagher, G. Koren, A. Gupta, and M. P. A. Fisher, Phys. Rev. Lett. **63**, 1511 (1989); **64**, 2586 (1990).

[64] J. R. Thompson, Y. R. Sun, L. Civale, A. P. Malozemoff, M. W. McElfresh, A. D. Marwick, and F. Holtzberg, Phys. Rev. B **47**, 14440 (1993).

[65] K. Yamafuji and T. Kiss, Physica C **258**, 197 (1996).

[66] T. Matsushita, T. Tohdoh, and N. Ihara, Physica C **259**, 321 (1991).

[67] M. Ziese, Phys. Rev. B **53**, 12422 (1996); **55**, 8106 (1997); Physica C **269**, 35 (1996).

[68] B. Roas, L. Schultz, and G. Saemann-Ischenko, Phys. Rev. Lett. **64**, 479 (1990).

[69] M. Fendorf, C. P. Burmester, L. T. Wille, and R. Gronsky, Appl. Phys. Lett. **57**, 2481 (1990).

[70] V. Svetchnikov, A. Palti, and V. Pan, Met. Phys. Adv. Tech. **17**, 257 (1998).

[71] V. Svetchnikov, V. Vysotskii, and V. Pan, Met. Phys. Adv. Tech. **17**, 1235 (1999).

[72] V. M. Pan, A. L. Kasatkin, V. L. Svetchnikov, V. A. Komashko, A. G. Popov, A. Yu. Galkin, H. C. Freyhardt, and H. W. Zandbergen, IEEE Trans. Appl. Supercond. **AS-9**, 1532 (1999).

[73] V. Selvamanickam, M. Mironova, S. Son, and K. Salama, Physica C **208**, 238 (1993).

[74] V. M. Pan, V. S. Flis, O. P. Karasevska, V. I. Matsui, I. I. Peshko, V. L. Svetchnikov, M. Lorenz, A. N. Ivanyuta, G. A. Melkov, E. A. Pashitskii, and H. W. Zandbergen, J. Superconductivity and Incorporated Magnetism **14**, 109 (2001).

[75] V. M. Pan, V. S. Flis, V. A. Komashko, O. P. Karasevska, V. L. Svetchnikov, M. Lorenz, A. N. Ivanyuta, G. A. Melkov, E. A. Pashitskii, and H. W. Zandbergen, IEEE Trans. Appl. Supercond. **AS-11**, 3960 (2001).

[76] V. M. Pan, A. L. Kasatkin, V. S. Flis, V. A. Komashko, V. L. Svetchnikov, A. G. Popov, A. V Pronin, O. P. Karasevska, C. L. Snead, M. Suenaga, and H. W. Zandbergen, Institute of Physics Conference Series No. 167, *Applied Superconductivity* (2000), p. 699.

[77] V. A. Komashko, A. G. Popov, V. L. Svetchnikov, A. V. Pronin, V. S. Melnikov, A. Yu. Galkin, V. M. Pan, C. L. Snead, and M. Suenaga, Semicond. Sci. Technol. **13**, 209 (2000).

[78] H. Safar, J. Y. Coulter, M. P. Maley *et al.*, Phys. Rev. B **52**, 9875 (1995).

[79] B. Meingast, O. Krant, T. Wolf, H. Wuehl, A. Erb, and G. Mueller-Vogt, Phys. Rev. Lett. **67**, 1639 (1991).

[80] U. Welp, M. Grimsditch, S. Fleshler, W. Nessler, B. Veal, and G. W. Crabtree, J. Supercond. **7**, 159 (1994).

[81] B. Meingast, A. Junod, and E. Walker, Physica C **272**, 106 (1996).

[82] A. Gurevich and E. A. Pashitskii, Phys. Rev. B **56**, 6213 (1997).

[83] J. B. Hirth and J. Lothe, *Theory of Dislocations*, McGraw-Hill, New York (1988).

[84] H. Ledbetter and M. Lei, J. Mater. Res. **6**, 2253 (1991).

[85] B. Dam, J. M. Huijbregtse, F. C. Klaassen, R. C. F. van der Geest, G. Doornbos, J. H. Rector, A. M. Testa, S. Freisem, J. C. Martinez, B. Staeuble-Puempin, and R. Griessen, Nature (London) **399**, 439 (1999).

[86] J. M. Huijbregtse, F. C. Klaassen, R. C. F. van der Geest, B. Dam, and R. Griessen, J. Low Temp. Phys. **32**, 114 (1999).

[87] L. Civale, A. D. Marwick, T. K. Worthington, M. A. Kirk, J. R. Thompson, L. Krusin-Elbaum, Y. Sun, J. R. Clem, and F. Holtzberg, Phys. Rev. Lett. **65**, 648 (1991).

Translated by Steve Torstveit